Thermographic Inspection of Bond Quality of FRP Strengthened Concrete

Chih-Hung CHIANG, Yu-Yuan LAIO, Wei-Hua YU
Chaoyang University of Technology, Wufong, Taichung 413
Chinese Taiwan
Phone: +886 4 23323000ext 4248, Fax: +886 4 23742325; e-mail: chiangc@cyut.edu.tw

Abstract

The bond quality is critical to stress transfer between fiber reinforced polymer, FRP, and concrete structures. The efficacy of externally bonded FRP systems could be reduced significantly due to defects at the FRP-concrete interface. Infrared thermography is an effective tool for locating such defects in a non-contact fashion. Current study examined the effects of size and depth of interface defects on surface temperature contrast. The sequence of defects appearing in a thermal image was determined by heat input and size and depth of defects collectively. Further analyses on the quantitative inspection are underway. Results of signal processing and image reconstruction will be presented.
Keywords: infrared thermography; FRP; bond quality

1. Introduction

The energy radiated from near the surface of any object can be detected using a thermographic camera in the infrared range of the electromagnetic spectrum, approximately 0.9 to 14μm. The amount of energy emitted by an object increases with temperature at a given wavelength, according to the black body radiation law. Hence the image produced by a thermographic camera can be used to detect the temperature difference at an object's surface. Such difference could be caused by the discontinuity in thermal characteristics inside an object or by the non-uniform heat transfer across the surface.

Infrared thermography is a non-contact technique that is suitable for inspecting subsurface defects of concrete plates and layered structures. The objective of the current study is to apply infrared thermography to inspect the interface de-lamination of carbon fiber reinforced polymer (CFRP) sheets bonded to a concrete substrate. Active sources including a halogen lamp arrays and a high-power flash had been applied to quickly heat the CFRP surfaces before the thermographic camera started to record thermal images. The air gaps between CFRP layers and those between CFRP and concrete slowed the heat flux and appeared as hot spots in the thermal images. Finite element models were constructed for analyzing transient temperature variations due to different boundary conditions.

2. Experimental program

The bonding quality of CFRP sheets onto a concrete substrate is usually dependent on the installation craftsmanship. American Concrete Institute specifies that de-laminations or air voids larger than 13cm^2 should be detected during quality inspection [1]. A circular area of 13cm^2 is equivalent to 4cm in diameter. Two concrete specimens were cast. Specimen no.1, shown in Figure 1, is 80cmX80cmX10cm with defects deliberately planted during installation of CFRP sheets. Specimens no.2 and no.3 are 40cmX60cm with different dimensions in thickness, as shown in Figures 2 and 3. All three specimens are covered with three layers of CFRP sheets. Some spots are left without primer and epoxy to simulate inferior bonding quality. Additional defects of various sizes are simulated using polymer films embedded between CFRP and concrete and between layers of CFRP. The thickness of simulated bonding defects is approximately 2mm.

The CFRP strengthened concrete specimens were subjected to different levels of heating using a long pulse or a simulated uniform source. The heating time of a long pulse is 1, 2, or 7 minutes respectively. Heating is provided using halogen lamps with power output ranging from 500 to 4500watts. The lamps are mounted on a sliding rack of a steel frame that enables back-and-forth movement to manually produce an approximately uniform heat flux. An array of flux meters attached to the CFRP surface provides measurements of actual heat flux received. These measurement results were used in the numerical models.

Thermal images were captured using an infrared camera, NEC TH7102. The minimum temperature difference detectable is 0.08^{o}C. The distance between the infrared camera and specimen no.1 is 2.5m. The distance between the infrared camera and specimen no.2 (no.3) is 0.75m.

Thermal images and thus surface temperatures were recorded for each specimen. The experimental procedure for specimens no.2 and no.3 also included data collection upon completion of the installation of one, two, and three CFRP sheets, respectively. The transient variation in surface temperatures can thus be analyzed for defects associated with each CFRP layer.

3. Numerical modeling

The transient heat equation for a large plate is given as

$$k\left(\frac{\partial^2 T}{\partial x^2}+\frac{\partial^2 T}{\partial y^2}\right)=\rho\ c\ \frac{\partial T}{\partial \tau} \qquad (1)$$

A two-dimensional finite element model was constructed using a software package ANSYS$^{@}$. A four-node plane element was selected with proper mesh sizes set for CFRP layers, air voids, the epoxy bonding layer, and the concrete substrate. The finest mesh used is 0.1mm such that a balance between accuracy and computing efficiency is achieved [2]. Heat flux, based on the measurements for each heating condition in the experimental program, was applied at the front surface of the top CFRP layer. Natural convection was allowed at the back surface of the concrete substrate.

4. Discussion

Transient temperature variations were obtained from both numerical models and IRT measurements. Both results showed similar trend in temperature contrast for large defects, 5cm and 10cm in diameter. However, the smallest defect, 2cm in diameter, was very difficult to detect due to insignificant temperature difference. Such conditions existed even for smallest defects near the surface, the interface between the top two layers of CFRP sheets. The results for specimen no.1 can be found in Figures 4 through 6, obtained using a 4500-watt heating source for one minutes.

The depth of the defects can be related to its transient visibility in the thermal images. For example, defects of the same size disappeared in sequence after heating had been terminated, as shown in Figure 7 and 8. The closer the defect to the surface, the sooner it would disappear in the thermal image. Heating conditions also have effects on such a sequence. Small defects embedded under three layers of CFRP after periodical pulsed heating tends to disappear more quickly than those under one or two layers of CFRP.

5. Defect sizing using edge detection technique

Defect sizing is important for assessment of CFRP bonding quality. There are various techniques that can be applied. For example, self-referencing and full-width half maximum were used in references [3-5] for processing thermal images of composite materials. Edge detection technique was applied in this study. It is based on maximum gradient of a grayscale image subject to computation of first-order derivatives of the surface temperature distribution. The calculation is relatively straightforward using digital filters and matrix operations [6]. The results for edge detection are given in Tables 1 and 2, for specimens no.2 and 3 respectively. Extracted defects are plotted in a binary image after the original thermal image is processed with the edge detection technique, as shown in Figure 9.

6. Concluding remark

Current study examined the effects of size and depth of interface defects on surface temperature contrast. Numerical modeling and IRT measurements were performed to analyze transient temperature variations due to defect characteristics and heating conditions. The following conclusions can be drawn from the current study.

(1) Temperature contrast of a thermal image is controlled by heating conditions, defect size, and defect depth.
(2) Defects of the same size disappeared in sequence after heating had been terminated. The closer the defect to the surface, the sooner it would disappear in the thermal image. Furthermore, the smaller the defect, the sooner it would disappear.
(3) Defects embedded between CFRP layers and between CFRP and the concrete substrate can be detected using IRT with proper heating conditions.
(4) Best results were produced in this study using a simulated uniform heating source. In some cases, periodical pulsed heating also achieved satisfactory images for subsurface defect.
(5) The lateral dimension of a defect can be effectively computed using the edge detection technique. Deviation from true defect diameters is within 20% for most cases.

Acknowledgements

This work is supported partly by National Science Council, project number NSC 96-2211-E324-022.

References

[1]. ACI 440.2R-02 Guide for the design and construction of externally bonded FRP systems for strengthening concrete structure.
[2]. Y-Y. Liaw and C-H. Chiang, Infrared inspection of CFRP-concrete plate bond characteristics, TCI 2007 Conference on Concrete Engineering, Taipei, Taiwan, November 2-3, 2007.
[3]. X. Maldague. Nondestructive Evaluation of Materials by Infrared Thermography. Springer-Verlag, London, 1993.
[4]. N.P. Avdelidis, D.P. Almond, Transient thermography as a through skin imaging technique for aircraft assembly: modelling and experimental results, Infrared Physics and Technology 45 (2004), 103-114.
[5]. M. Omar, M.I. Hassan, K. Saito, R. Alloo, IR self-referencing thermography for detection of in-depth defects, Infrared Physics and Technology 46 (2005), 283-289.

[6]. S.E. Umbaugh, Computer Vision and Image Processing: a Practical Approach Using CVIPtools. Prentice Hall, PTR, Upper Saddle River, New Jersey.

Table 1 Defect sizing results for specimen no.2. Simulated uniform heating for seven minutes were applied. Thermal image was acquired 10 second after heating had been terminated.

Algorithm of edge detection	No. of defect	True dimension		Estimated dimension		Deviation (%)	
		X(cm)	Y(cm)	X(cm)	Y(cm)	X	Y
Canny	1	2	2	2.2	2	-10	0
	2	2	2	2	1.8	0	10
	3	2	2	2	2	0	0
	4	5	5	4.4	5	12	0
	5	5	5	4.6	4.8	8	4
	6	5	5	4.6	5	8	0
Sobel	1	2	2	2.4	2	-20	0
	2	2	2	2	2	0	0
	3	2	2	2	2	0	0
	4	5	5	4.8	5.4	4	-8
	5	5	5	5.4	5	-8	0
	6	5	5	4.6	4.6	8	8

Table 2 Defect sizing results for specimen no.3. Periodical pulsed heating was applied for three minutes with a period of 10 seconds. Thermal image was acquired 10 seconds after the heating had been terminated.

Algorithm of edge detection	No. of defect	True dimension		Estimated dimension		Deviation (%)	
		X(cm)	Y(cm)	X(cm)	Y(cm)	X	Y
Canny	1	5	5	5	5.4	0	-8
	2	5	5	5.6	6	-12	-20
	3	5	5	5.4	6	-8	-20
	4	5	5	4.6	5	8	0
	5	2	2	1.2	*	40	*
	6	2	2	2	2	0	0
	7	2	2	2.2	1.4	-10	30
	8	2	2	2	*	0	*
Sobel	1	5	5	4.6	5.2	8	-4
	2	5	5	6	5.6	-20	-12
	3	5	5	5.6	5.8	-12	-16
	4	5	5	4.4	5	12	0
	5	2	2	*	*	*	*
	6	2	2	2.2	1.8	-10	10
	7	2	2	*	1.4	*	30
	8	2	2	*	*	*	*

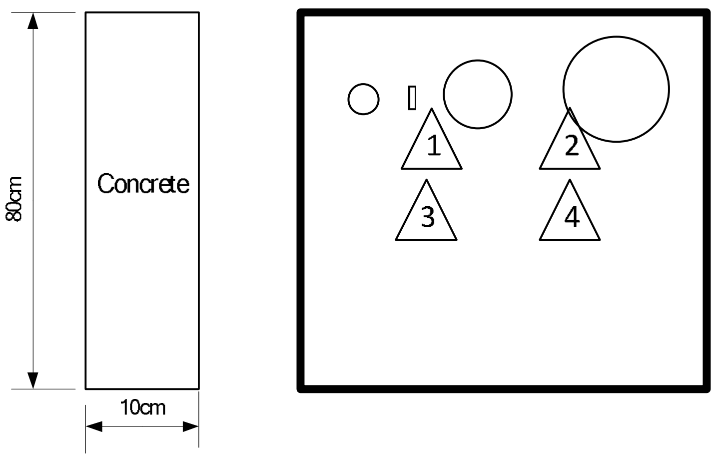

Figure 1 Dimension and defect configurations of specimen no.1. Triangular areas are left without primer and epoxy. Circular areas are embedded defects. ※ indicates a reference point of temperature.

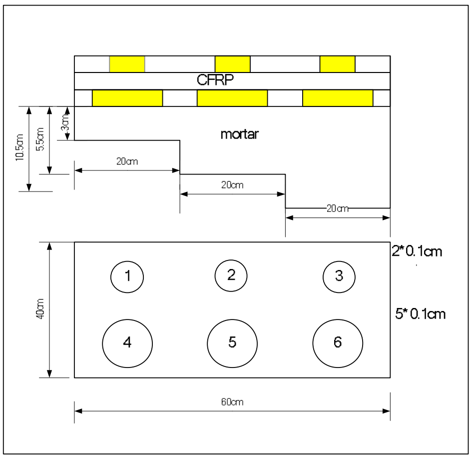

Figure 2 Dimension and defect configurations of specimen no.2.

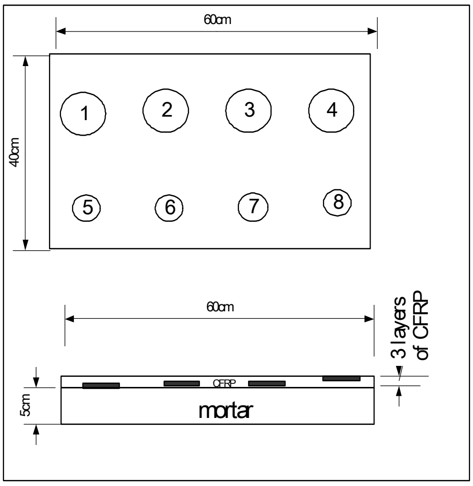

Figure 3 Dimension and defect configurations of specimen no.3.

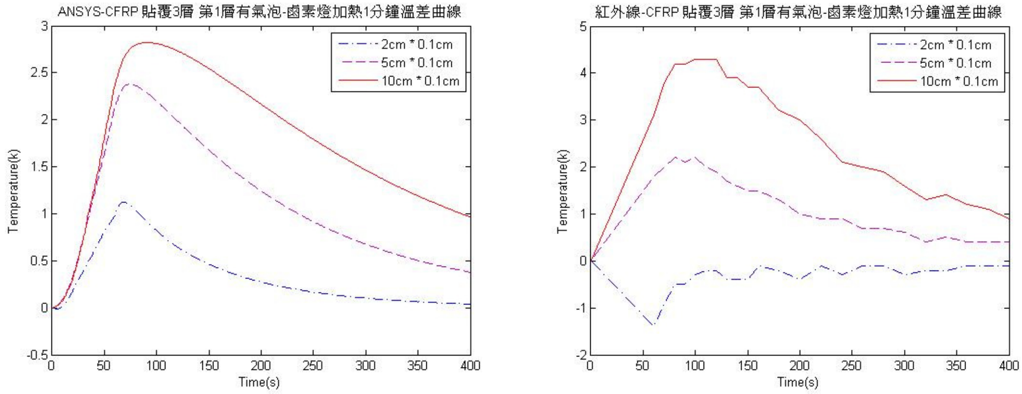

Figure 4 Temperature contrast of the interface between the first CFRP sheet and the concrete substrate obtained from numerical models (left) and IRT measurements (right). Legends indicate the size of defects.

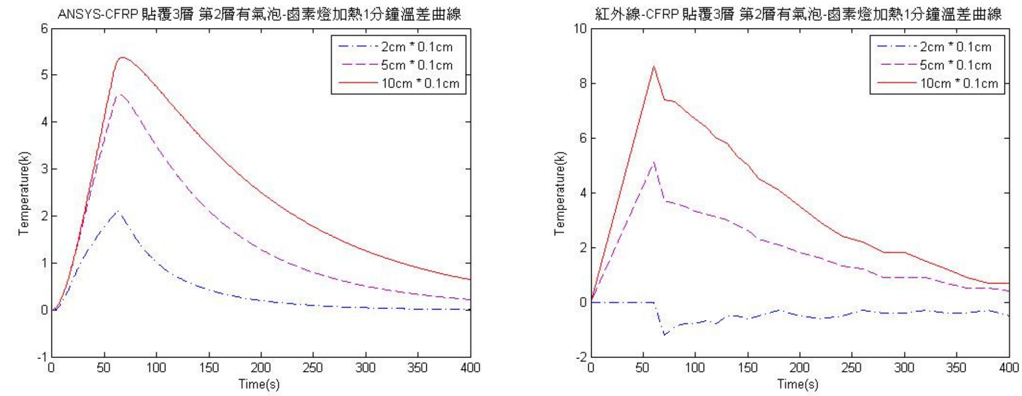

Figure 5 Temperature contrast of the interface between the first and the second CFRP sheets obtained from numerical models (left) and IRT measurements (right). Legends indicate the size of defects.

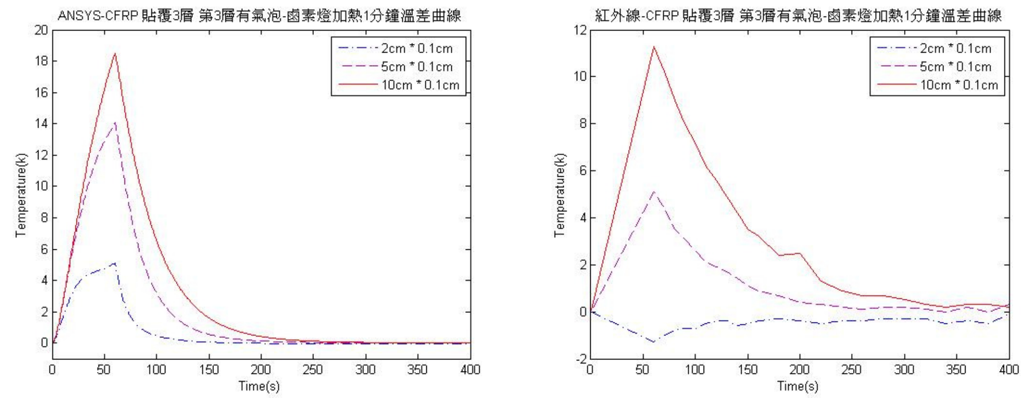

Figure 6 Temperature contrast of the interface between the second and the third CFRP sheets obtained from numerical models (left) and IRT measurements (right). Legends indicate the size of defects.

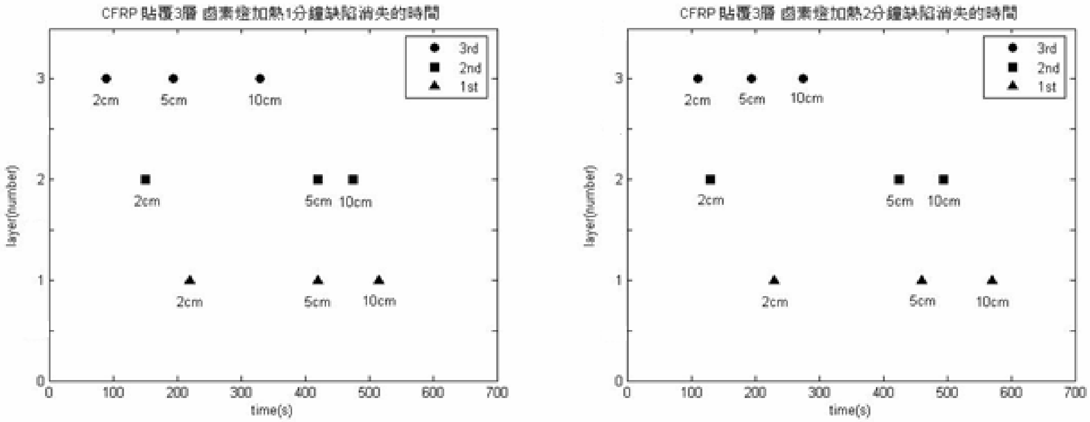

Figure 7 Transient visibility of defects in the thermal images of specimen no1 after heated for one minute (left) and two minutes (right). Defects of a diameter as indicated disappear at the time plotted in the figures. Legends also indicate the interface position of the defect, for example 3rd means the defect is in the interface between the second and the third layers of CFRP sheets.

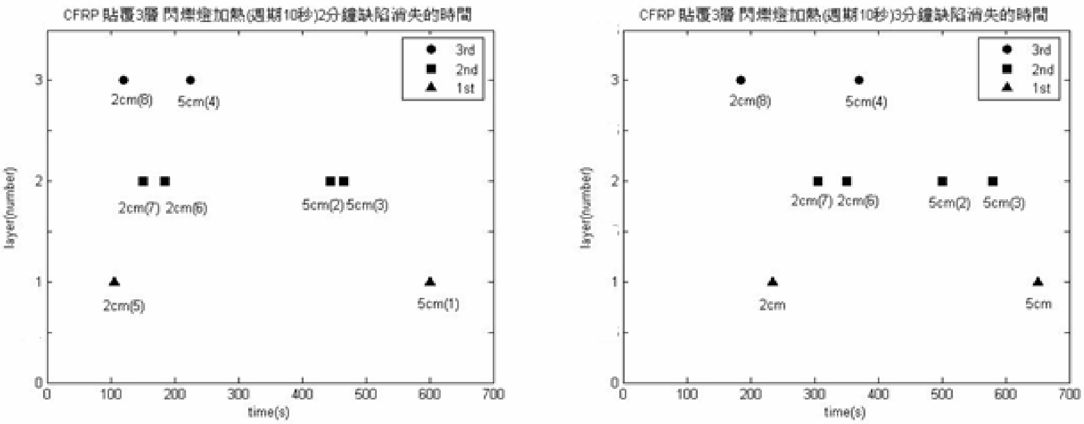

Figure 8 Transient visibility of defects in the thermal images of specimen no3 after heated for two minutes (left) and three minutes (right). Defects of a diameter as indicated disappear at the time plotted in the figures. Legends also indicate the interface position of the defect, for example 3rd means the defect is in the interface between the second and the third layers of CFRP sheets.

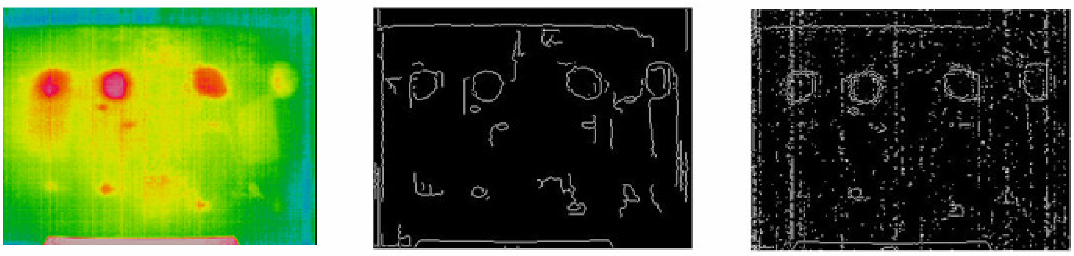

Figure 9 Examples of thermal image (left) and processed binary images (middle and right) of specimen no.3.